JOURNAL OF THERMOPHYSICS AND HEAT TRANSFER
Vol. 15, No. 3, July–September 2001

Technical Notes

TECHNICAL NOTES are short manuscripts describing new developments or important results of a preliminary nature. These Notes cannot exceed six manuscript pages and three figures; a page of text may be substituted for a figure and vice versa. After informal review by the editors, they may be published within a few months of the date of receipt. Style requirements are the same as for regular contributions (see inside back cover).

Pool Film-Boiling Heat Transfer from a Horizontal Downward-Facing Surface

Djati Walujastono,* Toshinori Okuda,*
and Kouichi Kamiuto†
Oita University, Oita 870-1192, Japan

Nomenclature

A = coefficient defined by Eq. (10)
B^* = dimensionless quantity defined by Eq. (18)
C_{PV} = specific heat at constant pressure, J/kg-K
C_0 = coefficient
D = diameter of the heated surface, m
E = coefficient
Gr = Grashof number, $g(\rho_L/\rho_V - 1)D^3/\nu_V^2$
g = gravitational acceleration, m/s^2
H = height of a heated surface extruded from the circumferential, insulated surface, m
H_W = immersion depth, m
$\bar{h}$ = heat-transfer coefficient, W/m^2-K
K^* = dimensionless quantity defined by $(1 + S_P/2)/S_P$
k_S = thermal conductivity of heated block, W/m-K
k_V = thermal conductivity of vapor, W/m-K
ℓ = latent heat of vaporization, J/kg
N_R = conduction-radiation parameter, $k_V/4\sigma T_w^3 D$
Nu = total Nusselt number, $\bar{h}D/k_V$
Pr_V = Prandtl number, $C_{PV}\mu_V/k_V$
q_c = convective heat flux, W/m^2-K
q_r = radiative heat flux, W/m^2-K
r = radial coordinate
r_0 = radius of the heated surface, $D/2$, m
S = dimensionless radius at the outer edge of a vapor film
S_P = dimensionless superheat, $C_{PV}\Delta T_{sat}/\ell$
s = radius at the outer edge of a vapor film, m
T = temperature, K
T_S = saturation temperature, K
T_w = temperature of the heated surface, K
u = velocity component in the radial direction, m/s
w = velocity component in the direction normal to the heated surface, m/s
X = film-boiling Rayleigh number, $Gr\,Pr_V K^*$
y = coordinate normal to the heated surface
α = absorptivity of the vapor-liquid interface ($\equiv 1$)
ΔT_{sat} = degree of wall superheat, $T_w - T_S$, K
ΔZ = distance between two adjacent thermocouples, m
δ = thickness of a vapor film, m
δ_0 = thickness of a vapor film at the center of the heated surface, m
ε = emissivity of the heated surface
η = dimensionless radius, $2r/D$
θ_s = dimensionless saturation temperature, T_s/T_w
μ_V = viscosity of vapor, $Pa - s$
ν_V = kinematic viscosity of vapor, m^2/s
ρ = density, kg/m^3
σ = Stefan–Boltzmman constant, W/m^2-K^4
ϕ = dimensionless thickness of a vapor film, $(\delta/D)^4(Gr\,Pr_V K^*/3)^{4/5}$

Subscripts

c = convective
l = liquid
r = radiative
v = vapor

Superscript

$\bar{}$ = mean value

Introduction

TO predict heat transfer characteristics of boiler water tubes, thermal characteristics of fuel rods under operation in emergency core cooling systems for light water reactors, and the quenching process of ferrous materials, better understanding of the mechanism of film boiling heat transfer and establishment of its theoretical models are necessary. In general, film-boiling heat transfer is significantly influenced by shape and orientation of the heated surfaces,[1–3] but, in the case of a horizontal surface facing downward, the heat-transfer coefficient is severely affected in an adverse manner. It is, therefore, important from the viewpoints of safety engineering and metallurgy to thoroughly clarify the heat transfer characteristics of film-boiling heat transfer from horizontal downward-facing surfaces and to establish the lower bounds of film-boiling heat transfer.

So far, a number of experimental studies[1–6] have been made on this subject using steady-state[1,2,6] or quenching[3–5] methods. The reported experimental data differ greatly between the experimental methods adopted and among the researchers. Generally, the Nusselt number obtained by the quenching method tends to decrease with film-boiling Rayleigh number X, whereas that determined by the steady-state heating method increases with X. Obviously, the difference observed between the heat transfer characteristics determined by the two methods is caused by the fact that the quenching method is concerned with transient (or unsteady) film boiling, whereas the steady-state heating method is not. Transient film boiling is of practical importance, but it is more difficult than steady-state film boiling to clarify the heat transfer mechanism and to establish a theoretical model. For this reason, in what follows, primary attention is focused on steady-state film boiling alone.

Recently, as for steady-state film boiling, Nishio et al.[6] suggested that the heat transfer coefficient can be augmented remarkably by disturbances caused by departing bubbles at the outer edge of a heated surface; and by suppressing this effect, they obtained experimental data for the heat transfer coefficient of stable pool-boiling heat transfer with a smooth vapor-liquid interface. Their data, however, covered a degree of wall superheat less than about 160 K, and thus the effect of radiation on film-boiling heat transfer can be fully disregarded. To our knowledge, there exist no experimental data for stable pool-film-boiling heat transfer from downward-facing

Received 5 June 2000; revision received 25 October 2000; accepted for publication 23 March 2001. Copyright © 2001 by the authors. Published by the American Institute of Aeronautics and Astronautics, Inc., with permission.

*Graduate Student, Department of Production Systems Engineering, Dannoharu 700.
†Professor, Department of Production Systems Engineering, Dannoharu 700; kamiuto@cc.oita-u.ac.jp. Senior Member AIAA.

surfaces with higher wall superheat. This is the case even for transient film boiling.

The aim of the present note is twofold: first, to conduct experiments for stable pool film-boiling heat transfer from horizontal downward-facing surfaces in the range of superheat greater than 200 K, corresponding to a film-boiling Rayleigh number less than about 10^{10}, and then to compare available heat transfer data determined by the steady-state heating method with the analytical predictions based on the one-equation boundary-layer integral method[5,6] taking into account the effect of radiation.

Experiment

Figure 1 shows a schematic diagram of the experimental apparatus used in the present study. The test vessel of 0.4 m in diameter and 0.245 m in height was made of stainless steel and contained distilled water kept at the saturation temperature at atmospheric pressure by means of auxiliary heaters. A brass cylinder was attached to the upper cover of the vessel, and its lower and side surfaces served as the heat-transfer sources. As seen from Fig. 1, the cylinder has a 0.06-m-diam flared top component coiled with a sheathed heater capable of producing a maximum heat flux of about 10^6 W/m^2 at the 0.03-m-diam heated bottom of the cylinder; and so the diameter of the heated surface D is 0.03 m. The height of the heated surface extruded from the circumferential, bakelite surface H was set at 0.003, 0.004, or 0.005 m using a screw mechanism attached to the upper cover of the vessel. Four K-type sheathed thermocouples of 0.001 m diam were embedded along the central axis of the cylinder to provide information on the axial temperature distribution and to permit determination of the surface temperature by extrapolation. This also allowed the surface heat flux to be estimated. In the experiment the brass cylinder was heated up to about 700 K, and then the water level in the vessel was increased and maintained at an immersion depth H_W of 0.001 m so as to suppress disturbances caused by departing bubbles. To estimate a gross magnitude of the heat loss from the uninsulated side surfaces, a heated surface with the side insulated ($H = 0.005$ m and $H_W = 0.001$ m) was also used. Furthermore, to follow the experiment of Ishigai et al.,[1] an additional experiment was performed under the condition of $H = 0$ and $H_W > 0.001$ m. The attainment of overall steady state was presumed when the rate of temperature change settled down below 2 K/hour, and this took about 3–6 hours. The axial temperature distribution of the brass cylinder and liquid temperature was continuously monitored using a personal computer and a chart recorder. The film-boiling behavior was photographed using a video camera. The electric current and voltage of the electric power supplied to the heater were measured using an ammeter and a voltmeter. The heat flux through the heat transfer surfaces q_W was computed from

$$q_W = \frac{\pi}{4} D^2 k_S \frac{\Delta T}{\Delta Z} \bigg/ \left(\frac{\pi}{4} D^2 + \pi D H_W \right) \tag{1}$$

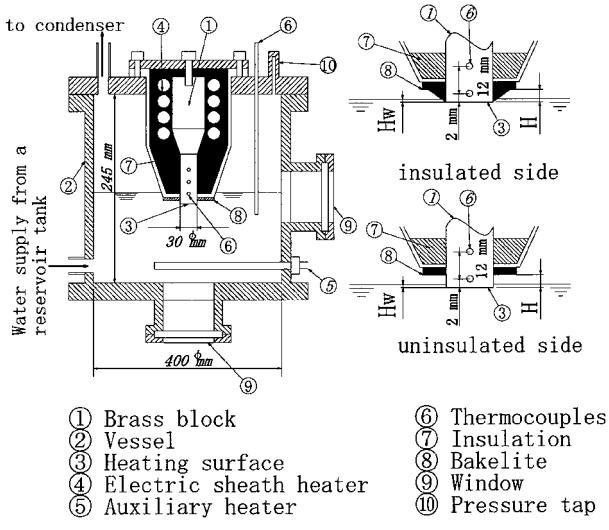

Fig. 1 Schematic diagram of the experimental apparatus.

where k_S is the thermal conductivity of brass. The heat flux at the heated surface was varied from 2×10^4 to 7×10^4 W/m^2, and the corresponding superheat was from 200 to 450 K. The Nusselt number was evaluated from

$$Nu = \frac{q_W D}{\Delta T_{\text{sat}} k_V} \tag{2}$$

Assuming negligible uncertainties associated with k_V and k_S, the relative uncertainty in Nu can be estimated as

$$\frac{\delta Nu}{Nu} = \left\{ \left(\frac{\delta \Delta T}{\Delta T} \right)^2 + \left(-\frac{\delta \Delta T_{\text{sat}}}{\Delta T_{\text{sat}}} \right)^2 + \left(-\frac{\delta \Delta Z}{\Delta Z} \right)^2 + \left[\frac{\delta (D - 4H_W)}{D - 4H_W} \right]^2 \right\}^{0.5} \tag{3}$$

Values for the individual relative uncertainty were estimated as $\delta \Delta T / \Delta T = \pm 0.104$, $\delta \Delta T_{\text{sat}} / \Delta T_{\text{sat}} \approx \delta \Delta T / \Delta T$, $\delta \Delta Z / \Delta Z = \pm 0.0021$, and $\delta (D - 4H_W)/(D - 4H_W) = \pm 0.0097$, and, upon substitution, we obtained $\pm 14.7\%$ as the resultant uncertainty in the Nusselt number.

Theoretical Analysis

The physical model for pool-film-boiling heat transfer and the coordinate system are shown in Fig. 2. The following assumptions are introduced for the analyses: 1) a stable vapor film is formed on the lower surface of the horizontal circular plate of diameter D and of uniform temperature T_w; 2) the vapor–liquid interface is smooth, and the effect of surface tension can be disregarded; 3) the vapor flow along the heat transfer surface is laminar; 4) the temperature distribution in the vapor film is linear; 5) the temperature at the vapor–liquid interface is equal to the saturation temperature T_S; 6) the radial velocity of the vapor at the vapor–liquid interface is zero; 7) the physical properties of the vapor are constant, and they are estimated at the film temperature; 8) the contribution of radiation heat transfer is considered, and the vapor is transparent to radiation, while the vapor–liquid interface is a blackbody surface.

The assumption of a linear temperature distribution[7] was proved to be quite reasonable as long as ΔT_{sat} is less than about 1000 K, but the assumption of zero radial velocity is somewhat arbitrary. However, this assumption is also acceptable because the effect of interface velocity on saturated film boiling heat transfer was found to be comparatively small.[8] Moreover, the vapor film thickness at the center of the heated surface was estimated to be less than 0.001 m even for $\Delta T_{\text{sat}} = 750$ K; hence, the use of the boundary-layer approximation can be fully justified in the present case.

Under these assumptions, the boundary conditions for the vapor film are given as follows:

$$y = 0: \quad u = 0, \quad T = T_w \tag{4}$$

$$y = \delta: \quad u = 0, \quad T = T_S \tag{5}$$

$$r = 0: \quad \frac{d\delta}{dr} = 0 \tag{6}$$

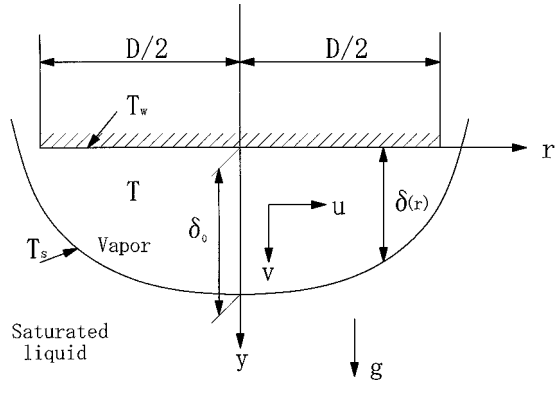

Fig. 2 Physical model and the coordinate system.

$$r = s\left(>\frac{D}{2}\right): \qquad \delta = 0, \qquad \frac{\mathrm{d}\delta}{\mathrm{d}r} = -\infty \tag{7}$$

The velocity profile of the vapor film is written as

$$u = A\delta^2[(y/\delta) - (y/\delta)^2] \tag{8}$$

and the momentum equation for the vapor in the radial direction is given by

$$\mu_V \frac{\mathrm{d}^2 u}{\mathrm{d}y^2} = (\rho_L - \rho_V) g \frac{\mathrm{d}\delta}{\mathrm{d}r} \tag{9}$$

Substituting Eq. (8) into Eq. (9), we can obtain

$$A = -\left[\frac{g(\rho_L - \rho_V)}{2\mu_V}\right]\left(\frac{\mathrm{d}\delta}{\mathrm{d}r}\right) \tag{10}$$

On the other hand, the temperature distribution within the vapor film can be written as

$$T = T_w - \Delta T_{\mathrm{sat}}(y/\delta) \tag{11}$$

Moreover, from the assumptions (7) and (8), the integral energy equation of the vapor film results in

$$-rk_V\left(\frac{\partial T}{\partial y}\right)_{y=0} + rq_r = \frac{\mathrm{d}}{\mathrm{d}r}\left[\rho_V C_{\mathrm{PV}} r \int_0^\delta u\left(T - T_S + \frac{\ell}{C_{\mathrm{PV}}}\right)\mathrm{d}y\right]$$

$$= \frac{\mathrm{d}}{\mathrm{d}r}\left\{\rho_V \delta l r \int_0^1 u[(1 + S_P) - \eta S_P]\,\mathrm{d}\eta\right\} \tag{12}$$

where

$$q_r = \frac{\sigma\left(T_w^4 - T_s^4\right)}{(1/\varepsilon + 1/\alpha - 1)} \tag{13}$$

$$S_P = C_{\mathrm{PV}}\Delta T_{\mathrm{sat}}/\ell \tag{14}$$

Substituting Eqs. (8), (10), (11), (13), and (14) into Eq. (12) and using the dimensionless quantities defined by Eq. (16) yields the following governing equation for the vapor film thickness δ:

$$\frac{\mathrm{d}}{\mathrm{d}r}\left(r\frac{\mathrm{d}\delta^4}{\mathrm{d}r}\right) + \left(\frac{r}{\delta}\right)\frac{48D^3}{Gr\,Pr_V K^*}$$

$$= -12rD^2\frac{\left(1 + \theta_S + \theta_S^2 + \theta_S^3\right)}{Gr\,Pr_V K^* N_R(1/\varepsilon + 1/\alpha - 1)} \tag{15}$$

$$Gr = \frac{g(\rho_L/\rho_V - 1)D^3}{\nu_V^2}, \qquad Pr_V = \frac{\mu_V C_{\mathrm{PV}}}{k_v}$$

$$N_R = \frac{k_V}{4\sigma T_w^3 D}, \qquad K^* = \frac{(1 + S_P/2)}{S_P} \tag{16}$$

Introducing the dimensionless radial coordinate $\eta(=2r/D)$ and dimensionless vapor film thickness $\phi[=(\delta/D)^4\,(Gr\,Pr_v K^*/3)^{4/5}]$, we can rewrite Eq. (15) as

$$\frac{\mathrm{d}}{\mathrm{d}\eta}\left[\eta\left(\frac{\mathrm{d}\phi}{\mathrm{d}\eta}\right)\right] + \frac{4\eta}{\phi^{0.25}} = -B^*\eta \tag{17}$$

Here, the dimensionless quantity B^* is defined by

$$B^* = \frac{1}{N_R}\left(\frac{3}{Gr\,Pr_V K^*}\right)^{0.2}\frac{1 + \theta_s + \theta_s^2 + \theta_s^3}{1/\varepsilon + 1/\alpha - 1} \tag{18}$$

Next, we assume that ϕ can be written in the following form[6]:

$$\phi = E(S - \eta^2)^n \tag{19}$$

In accordance with Nishio et al.,[6] the values of S and n are taken as 1.01 and 1, respectively. On the basis of the Ritz method, the parameter E in Eq. (19) can be determined from

$$E^{\frac{5}{4}}\left[4\int_0^1 (S - \eta^2)\,\mathrm{d}\eta\right] - 4\int_0^1 (S - \eta^2)^{\frac{3}{4}}\,\mathrm{d}\eta$$

$$- E^{\frac{1}{4}}\left(B^*\int_0^1 (S - \eta^2)\,\mathrm{d}\eta\right) = 0 \tag{20}$$

This equation shows that E is a function of B^*. Obviously, Eq. (20) cannot be solved analytically with respect to E, and thus we must resort to a numerical means: the bisection method was adopted here. The obtained numerical results were approximated by

$$E = \frac{1.05609 + 0.30616B^* + 0.024901B^{*2}}{1 + 0.1005627B^*} \tag{21}$$

When radiation does not participate in heat transfer, that is, $B^* = 0$, E takes a value of 1.05609. Moreover, it is found that E is an increasing function of B^*, and thus the vapor film thickness increases with the heating surface temperature T_W.

The total heat transfer coefficient $\bar{h}$ is represented by a sum of the convective heat transfer coefficient $\bar{h}_c$ and the radiative heat transfer coefficient $\bar{h}_r$.

$$\bar{h} = \bar{h}_c + \bar{h}_r \tag{22}$$

$$\bar{h}_c = \frac{q_c}{\Delta T_{\mathrm{sat}}} = \frac{2k_v}{r_0^2}\int_0^{r_0}\frac{r\,\mathrm{d}r}{\delta} \tag{23}$$

$$\bar{h}_r = \frac{q_r}{\Delta T_{\mathrm{sat}}} = \frac{\sigma\left(T_w^4 - T_S^4\right)}{\Delta T_{\mathrm{sat}}(1/\varepsilon + 1/\alpha - 1)} \tag{24}$$

The total Nusselt number Nu is also represented by a sum of the convective Nusselt number Nu, c and the radiative Nusselt number Nu, r:

$$Nu = Nu, c + Nu, r \tag{25}$$

$$Nu, c = \frac{\bar{h}_c D}{k_v} = \frac{4}{r_0}\int_0^{r_0}\frac{r\,\mathrm{d}r}{\delta}$$

$$= \left[\frac{2}{3^{0.2}}\frac{1}{E^{0.25}}\int_0^1 \frac{\eta\,\mathrm{d}\eta}{(1.01 - \eta^2)^{0.25}}\right]X^{0.2} = C_0 X^{0.2} \tag{26}$$

$$C_0 = \frac{1.04485}{E^{0.25}} \tag{27}$$

$$Nu, r = \frac{\bar{h}_r D}{k_v} = \frac{1 + \theta_s + \theta_s^2 + \theta_s^3}{4N_R(1/\varepsilon + 1/\alpha - 1)} = \frac{B^*}{4}\left(\frac{X}{3}\right)^{0.2}$$

$$= 0.2007B^* X^{0.2} \tag{28}$$

When $B^* = 0$, C_0 becomes 1.03, which is very close to the value obtained by Nishio et al.,[6] that is, $C_0 = 1.02$. It should be stressed here that Nu, c involves the effect of radiation through E, and, therefore, Nu, c decreases with an increase in radiation. However, detailed inspection of the theoretically obtained Nusselt number Nu indicates that, for constant X, Nu increases with an increase in radiation, which can be realized by decreasing N_R and/or increasing θ_s. Shigechi et al.[9] have made a theoretical analysis based on the two-equation boundary-layer integral method, where the vapor-film thickness and representative radial velocity were treated as unknowns and the effect of radiation was considered, but they did not derive any analytical expressions for heat-transfer correlation; thus, the present theoretical results, namely, Eqs. (25–28), could not be compared with their results.

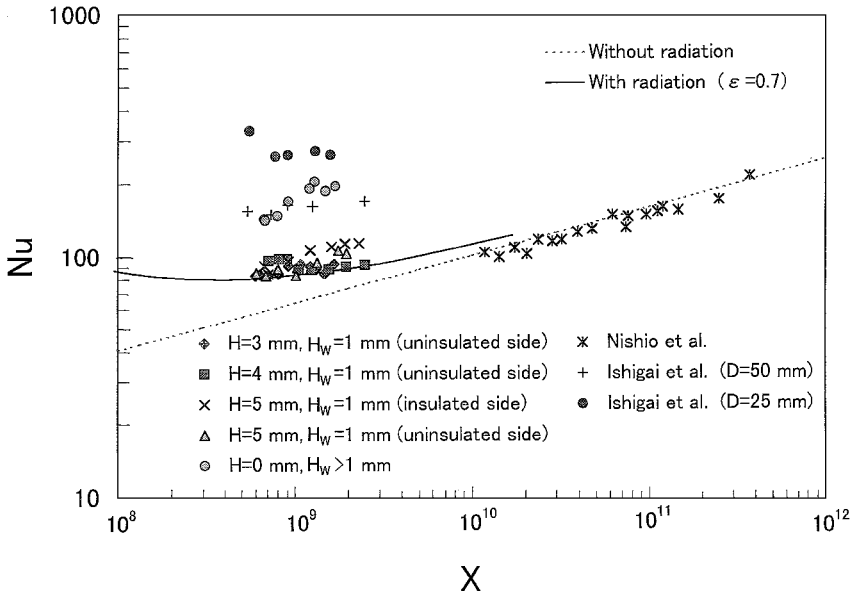

Fig. 3 Relations between the total Nusselt number *Nu* and the film-boiling Rayleigh number *X*.

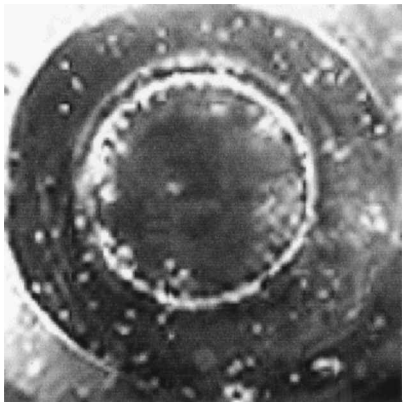

$H = 0.003$ m and $H_W = 0.001$ m ($q_W = 5.5 \times 10^4$ W/m^2)

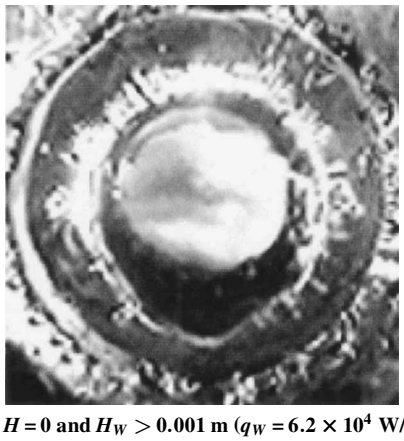

$H = 0$ and $H_W > 0.001$ m ($q_W = 6.2 \times 10^4$ W/m^2)

Fig. 4 Photographs of the behavior of film boiling from the downward-facing heated surfaces.

Results and Discussion

The obtained experimental results are summarized in Fig. 3, where the vertical axis represents *Nu*, while the horizontal axis denotes X. Values of the relevant physical properties were estimated at the film temperature, namely, $(T_w + T_S)/2$. The experimental data for steady-state film-boiling heat transfer reported by Ishigai et al.[1] and Nishio et al.[6] are depicted on the same figure. Ishigai et al.[1] utilized copper test sections of $H = 0$ and $H_W = 0.025$ m, whereas Nishio et al.[6] performed experiments using polished aluminum plates of $H = 0.006$ m and $H_W = 0.003$ m.

The present results except for $H = 0$ and $H_W > 0.001$ m are much lower than those reported by Ishigai et al., and, at the same time, our data for $H = 0$ and $H_W > 0.001$ m are located between the data of Ishigai et al. for $D = 0.025$ and 0.05 m. This fact strongly suggests that their experimental data were fully affected by disturbances caused by departing bubbles at the outer edge of the heated surface, whereas, in our cases except for the heated surface of $H = 0$ and $H_W > 0.001$ m, the film boiling heat transfer was scarcely affected by departing bubbles; hence, quite stable film boiling was realized. This conjecture is supported by comparison of a photograph of film boiling from the heated surface of $H = 0.003$ m ($H_W = 0.001$ m) with that of $H = 0$ ($H_W > 0.001$ m) in Fig. 4, which was taken from video frames. Moreover, there exists little difference between the heat transfer coefficients for the test sections with and without side insulation. This indicates the gross magnitude of the heat loss of the uninsulated side surfaces, which was estimated to be 4.1–12.1%.

Theoretical results for perfectly reflecting surfaces ($\varepsilon = 0$ and $C_0 = 1.02$) and the oxidized brass surfaces[10] ($\varepsilon = 0.7$) are indicated by the broken and solid lines, respectively, in Fig. 3. Agreement between the predictions and the experimental results is satisfactory: the present formula approximates 92.2% of the available data with an error of less than ±20%.

Conclusions

The results obtained here can be summarized as follows:

1) Experimental data of stable pool-film-boiling heat transfer from downward-facing surfaces in the range of film-boiling Rayleigh number less than about 10^{10} were obtained by keeping the height of the heated surface large while holding the immersion depth at a minimum.

2) The heat transfer correlation derived from the one-equation boundary-layer integral method by taking into account the effect of radiation reproduces the existing stable film-boiling heat transfer data obtained by the steady-state heating method with an acceptable accuracy.

References

[1] Ishigai, S., Inoue, K., Kiwaki, Z., and Inai, T., "Boiling Heat Transfer from a Flat Surface Facing Downward," *International Developments in Heat Transfer*, American Society of Mechanical Engineers, New York, 1961, pp. 224–229.

[2] Seki, N., Fukusako, S., and Torikoshi, K., "Experimental Study on the Effect of Orientation of Heating Circular Plate on Film Boiling Heat Transfer for Fluorocarbon Refrigerant R-11," *Journal of Heat Transfer*, Vol. 100, No. 4, 1978, pp. 624–628.

[3]Guo, Z., and El-Genk, M. S., "An Experimental Study of Saturated Pool Boiling from Downward Facing and Inclined Surfaces," *International Journal of Heat and Mass Transfer*, Vol. 35, No. 9, 1992, pp. 2109–2117.

[4]Yamada, T., Shigechi, T., Momoki, S., and Kanemaru, K., "Heat Transfer Correlation of Film Boiling from a Downward-Facing Horizontal Circular Plate," *Heat Transfer-Japanese Research*, Vol. 26, No. 7, 1997, pp. 459–468.

[5]Barrow, R. F., and Dergham, A. R., "Film Boiling to a Plate Facing Downward," *Advances in Cryogenics*, Vol. 33, 1987, pp. 355–362.

[6]Nishio, S., Himeji, Y., and Dhir, V. K., "Natural-Convection Film Boiling Heat Transfer: Second Report, Film Boiling from a Horizontal Flat Plate Facing Downward," *Proceedings of the American Society of Mechanical Engineers/Japan Society of Mechanical Engineers Thermal Engineering Conference*, Vol. 2, American Society of Mechanical Engineers, New York, 1991, pp. 275–280.

[7]Walujastono, D., and Kamiuto, K., "Pool Film Heat Transfer from a Horizontal Circular Plate Facing Downward," *Nippon Kikaigakai Ronbunshu (Series B)*," Vol. 65, No. 637, 1999, pp. 3091–3096.

[8]Nishikawa, K., and Ito, T., "Two-Phase Boundary-Layer Treatment of Free-Convection Film Boiling," *International Journal of Heat and Mass Transfer*, Vol. 9, No. 1, 1966, pp. 103–115.

[9]Shigechi, T., Kawae, N., Tokita, Y., and Yamada, T., "Film Boiling Heat Transfer from a Horizontal Circular Plate Facing Downward," *JSME International Journal*, Vol. 32, No. 4, 1989, pp. 646–651.

[10]Touloukian, Y. S. (ed.), *Thermophysical Properties of High Temperature Solid Materials*, Vol. 2, Macmillan, New York, 1967, pp. 180, 181.

Positivity of Entropy Production and Phase Density in the Chapman–Enskog Expansion

Henning Struchtrup*
Arizona State University, Tempe, Arizona 85282-1804

Nomenclature

C_k	=	peculiar velocity, $c_k - v_k$, m/s
$C_{\max}$	=	upper bound for peculiar velocity, m/s
c_k	=	microscopic velocity, m/s
f	=	phase density, s^3/m^6
f_M	=	Maxwell distribution, s^3/m^6
Kn	=	Knudsen number, $\eta/Lp\sqrt{(k/m)T}$
k	=	Boltzmann's constant, 1.3804×10^{-23} J/K
L	=	typical length scale, m
m	=	particle mass, kg
p	=	pressure, N/m^2
$\mathcal{S}$	=	collision term, s^2/m^6
T	=	temperature, K
t	=	time, s
v_i	=	center of mass velocity, m/s
x_k	=	space variable, m
$\partial v_{\langle i}/\partial x_{j\rangle}$	=	symmetric and trace free part of the velocity gradient, 1/s
η	=	viscosity, kg/ms
ξ	=	dimensionless velocity
ρ	=	mass density, kg/m^3
σ	=	entropy production, J/K
Φ	=	nonequilibrium part of phase density
$\phi^{(n)}$	=	expansion coefficients of Φ

Introduction

IN a recent paper Comeaux et al.[1] showed that the entropy production according to the Burnett equations may become negative. This result stands in contradiction to Boltzmann's H-theorem, which states that the entropy production is positive for any distribution function f. In this Note we show that the negative production of entropy results from the use of approximative solutions of the Boltzmann equation outside their proper range and improper mathematics, that is, a series expansion that does not converge outside that range.

The behavior of rarefied gases is well described by the Boltzmann equation[2,3]

$$\frac{\partial f}{\partial t} + c_k \frac{\partial f}{\partial x_k} = \mathcal{S} \tag{1}$$

where f is defined such that $f\,\mathrm{d}\boldsymbol{c}\,\mathrm{d}\boldsymbol{x}$ gives the number of particles with velocities in $(c_i, c_i + \mathrm{d}c_i)$ in the space element $(x_i, x_i + \mathrm{d}x_i)$ at time t. The collision term $\mathcal{S}(f, f)$ describes the change of f as a result of collisions among the particles; the particular form of $\mathcal{S}$ can be found in the literature.[2,3]

Being a nonlinear integro-differential equation, the Boltzmann equation cannot be solved analytically and must either be treated numerically or with approximations. The latter is usually done by the Chapman–Enskog method[3] or by Grad's moment method.[4,5]

The Chapman–Enskog method uses a series expansion into powers of the Knudsen number Kn, with the Euler equations as solution of order zero, the Navier–Stokes equation as first-order correction, and the so-called Burnett equations for the second-order approximation. Thus, from the derivation it is clear that the equations—Euler, Navier–Stokes, or Burnett—have only a finite range of applicability (defined by the Knudsen number) and cannot serve for the description of any processes in a gas. Besides, the Burnett equations become unstable for steep gradients.[6]

Boltzmann's celebrated H-theorem[2,3] states that the entropy production

$$\sigma = -k \int \mathcal{S}\, \ln f\, \mathrm{d}\boldsymbol{c} \tag{2}$$

is positive for all phase densities f. The proof relies on the particular form of the collision term $\mathcal{S}$ and can be found in the cited literature.

Thus, the findings in Ref. 1, a negative entropy production, are in contradiction to the H-theorem. This discrepancy will be discussed in the following.

Positivity of Phase Density and Entropy Production

The Chapman–Enskog method is an expansion in terms of the Knudsen number Kn, which gives the ratio between the mean free path of a gas particle and a typical macroscopic length scale. The method yields the phase density[2,3]

$$f = f_M(1 + \Phi) \qquad \text{where} \qquad \Phi = Kn\phi^{(1)} + Kn^2\phi^{(2)} + \cdots \tag{3}$$

$$f_M = (\rho/m)\sqrt{m/2\pi kT}^{\,3} \exp[-(m/2kT)C^2] \tag{4}$$

The $\phi^{(n)}$ are products between polynomials in the peculiar velocity and derivatives in space and time of temperature and velocity.[3] The simplest example is given by the first Chapman–Enskog expansion for Maxwell molecules where[3,1]

$$\Phi = -\frac{\eta}{p(k/m)T} C_i C_j \frac{\partial v_{\langle i}}{\partial x_{j\rangle}} + \frac{15}{4}\frac{\eta}{pT}\left(1 - \frac{1}{5}\frac{m}{kT}C^2\right) C_k \frac{\partial T}{\partial x_k} \tag{5}$$

The phase densities for higher-order expansions (Burnett, Super-Burnett) can be found in the literature.

Because of its definition as a number density in phase space, the phase density ought to be positive, and, moreover, the definition in Eq. (2) only makes sense for positive f. The Chapman–Enskog expression, Eq. (3), however, will become negative because Φ will fall below (-1) for large C.

In the proper range of applicability, the gradients of temperature and velocity are rather small, and Φ falls below (-1) only for very large C. However, Φ is always multiplied by the Maxwellian (4),

Received 14 March 2000; revision received 27 November 2000; accepted for publication 18 December 2000. Copyright © 2001 by the American Institute of Aeronautics and Astronautics, Inc. All rights reserved.

*Visiting Professor, Department of Mathematics; struchtr@ima.umn.edu; currently Assistant Professor, Department of Mechanical Engineering, University of Victoria, Victoria, British Columbia, V8W 3P6, Canada; struchtr@me.uvic.ca.